DE GRUYTER Sci Eng Compos Mater 2018; 25(5): 957–961

Kaiyue Wang*, Huijun Wang, Yi Zhou, Guomin Li, Yaqiao Wu, Jianying Hao and Yuming Tian

Preparation and characterization of low-cost high-performance mullite-quartz ceramic proppants for coal bed methane wells

https://doi.org/10.1515/secm-2017-0142
Received April 21, 2017; accepted August 27, 2017; previously published online October 17, 2017

Abstract: In this study, the mullite-quartz-based proppants were successfully prepared by using the coal gangue as the raw materials. Then, the effects of the additive and the sintering temperature on the composition, microstructure, and properties of the proppants were investigated. Results showed that the proppants sintered at 1250°C with the 10 wt% bauxite additive presented the best performance, which was very close to that of the quartz-proppant, and met the operational requirements of the 52 MPa coal bed methane wells. The viscous flow mechanism of the liquid phase formed during the sintering process also promoted the arrangement of the grains, thus benefiting the densification and the strength of the proppants.

Keywords: microstructure; proppants; sintering; strength.

1 Introduction

The coal bed methane (CBM), is an economically important unconventional fossil energy resource that attracts much scientific and industrial interest [1]. When the air concentration of the CBM exceeds 5%, it tends to explode in the case of fire. Therefore, the CBM must be exploited before performing coal mining. During the exploitation of the CBM, the hydraulic fracturing technology is one of the effective measures used to enhance industrial production [2, 3]. In the process of hydraulic fracturing, the proppants consist of spherical ceramic particles, which can resist the fracture closure to create the gas channel. Therefore, their performance directly determines the CBM recovery. As the main raw material of proppant preparation, bauxite has become scarce and expensive [4]; thus, the need for a replacement is increasingly urgent.

Compared with oil exploration, the CBM is located at the shallower and softer stratum, resulting in lower requirements for the packing density and the crush ratio of the proppants [5, 6]. Hereby, a mineral with less Al_2O_3 is a better selection to reduce the production costs compared with other options. As a major solid waste in Shanxi Province, China, coal gangue (~20.7 wt% Al_2O_3) has been used mainly for building cement but rarely for ceramics [7]. In this paper, low-cost proppants were successfully prepared by using the raw materials of coal gangue, together with bauxite as an additive. Furthermore, the effects of the additive and the sintering temperature on the phase composition, microstructure, and properties of the proppants were investigated.

2 Materials and methods

2.1 Raw materials

The starting materials were coal gangue with bauxite as the additive, which were supplied by the Changqing Fracturing Proppant Co. Ltd., Yangquan, Shanxi, China. The coal gangue consisted of 27.4 wt% Al_2O_3, 8.1 wt% Fe_2O_3, 30.7 wt% SiO_2, 2.7 wt% TiO_2 and 31.1 wt% others, and the loss on ignition was 25.4 wt%. The chemical composition analysis of the bauxite powder was as follows: 60 wt% Al_2O_3, 13.8 wt% SiO_2, and 26.2% other oxides.

2.2 Experimental procedure

The coal gangue, together with the bauxite ores as the additive, were crushed into millimeter-scaled particles, respectively, by a Jaw crusher and were milled further to amicrometer-size by a roll crushing mill and a QLM series jet airflow mill. The amounts of additives were 0 wt%, 5 wt%, 10 wt%, 15 wt% and 20 wt%, respectively. Homogeneous mixtures were obtained by ball-milling in

---

***Corresponding author: Dr. Kaiyue Wang,** School of Materials Science and Engineering, Taiyuan University of Science and Technology, 66 Waliu Road, Wanbolin District, Taiyuan 030024, Shanxi Province, China, Phone: +86 13753184246, e-mail: wangkaiyue8@163.com
Huijun Wang, Yi Zhou, Guomin Li, Yaqiao Wu, Jianying Hao and Yuming Tian: School of Materials Science and Engineering, Taiyuan University of Science and Technology, Taiyuan 030024, Shanxi Province, China

an absolute ethanol medium for 6 h and then drying in a DH-101-2BS oven (Experimental Central Electric Furnace Co., Ltd. Tianjin, Chian) at 120°C for 36 h. The dried lumps were crushed, sieved through screening (100 μm mesh) to break up the agglomerates, and then placed into an R02 Eirich granulator (Eirich Group, Germany) machine to form spherical green bodies, with 10 wt% 5 g/mL polyvinyl alcohol solution as the temporary binder. Afterwards, the green bodies were dried at 120°C for 5 h and then sintered in a KBF 1700 electric furnace (Nanjing Boyun Instrument Technology Co., Ltd, Nanjing, China) in air at 1100°C, 1150°C, 1200°C, 1250°C and 1300°C and at holding times of 2 h, respectively. Finally, the samples were cooled down to 400°C at a cooling rate of 5°C/min and furnace-cooled to room temperature. The as-sintered spherical proppants, with diameters of 212–425 μm, were collected successively through 40 and 70 mesh.

2.3 Characterization

The packing density, apparent density, and the crush ratio under 52 MPa pressure were determined in accordance with the Petroleum and Gas Industry Standard SY/T 5108-2014. The packing density is given by $\rho_V=(m_2-m_1)/V$; where m_1 is the mass of the density bottle, m_2 is the mass of the density bottle filled with proppants, and V is the volume of the density bottle. The apparent density was measured by Archimedes' method. This is calculated by using the formula $\rho_a=(m_2-m_1)/(V-V_w)$; where V_w is the volume of water when the density bottle is filled with proppants and water. The crush ratio was tested by the die-crushing chamber, with a diameter of 50.8 mm. This is calculated by using the formula $\eta=\mathrm{W_c}/\mathrm{W_0}\times 100\%$; where $\mathrm{W_0}$ is the weight of the as-examined specimens; and Wc is the weight of the crushed specimens after testing. The values of the results were obtained from a five-time average.

The microscopic morphology of the fractured surface of as-sintered proppants was observed by field-emission scanning-electron microscopy (SEM, S4800, Hitachi Ltd, Tokyo, Japan.). X-ray powder diffraction (XRD, Philips Co. Ltd, Amsterdam, Holland) was performed to identify the phase composition of the specimens by using Ni-filtered Cu Kα radiation with a scanning speed of 0.02°/step. The thermal properties of the raw materials were studied simultaneously by thermogravimetry (TG) and differential-scanning calorimetry (DSC) (Mettler Toledo, Zurich, Switzerland). The test was performed from 50°C–1300°C at a flowing nitrogen atmosphere with a heating rate of 10°C/min.

3 Results and discussion

The TG-DSC results of the coal gangue are shown in Figure 1. Weight loss of the gangue mainly occurred from 350°C–900°C. A wide endothermic peak of the DSC curve was observed in the range of 200°C–400°C, which might have been caused by the loss of free and adsorbed water. With the increase in temperature, weight loss was 21.8%, and a valley appeared at approximately 510°C, which was caused by the combustion of residual coal in the gangue. Weight loss between 890°C–1067°C was slight; however, abundant reactions and phase changes occurred. The metakaolinite decomposed into the amorphous Al_2O_3 and SiO_2 before 976°C [8, 9], after which, rod-like mullite ($3Al_2O_3\cdot 2SiO_2$) appeared as the temperature increased [10, 11]. Therefore, in our research, the samples were first heated to 300°C at 5°C/min, held for 30 min to remove the water vapor, and then heated to 650°C at 2°C/min and held again for 30 min to eliminate the residual coal. Moreover, the sintering temperature was defined as higher than 1067°C to obtain a high-strength and high-toughness mullite phase.

The only starting material of coal gangue failed to form spherical particles. Therefore, the bauxite powder was added as an additive to improve the plasticity of the raw materials and the strength of the sintered proppants. Figure 2 shows the crush ratio under a 52 MPa closure pressure for the 40/70 mesh proppants sintered at 1200°C with different amounts of the bauxite additive. As can be seen, when the amount of bauxite increased, the crush ratio decreased, and the cost for the proppants increased.

The results also showed that the crush ratio of proppants with 10 wt% additives was just lower than 10%, and this value was very close to that of the quartz-proppant,

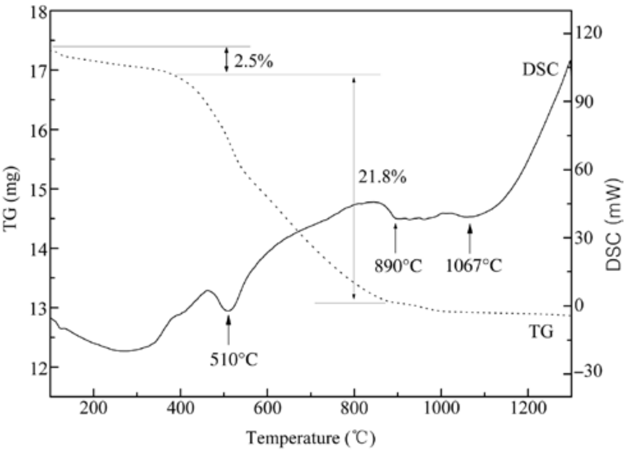

Figure 1: The TG-DSC curves of the coal gangue.

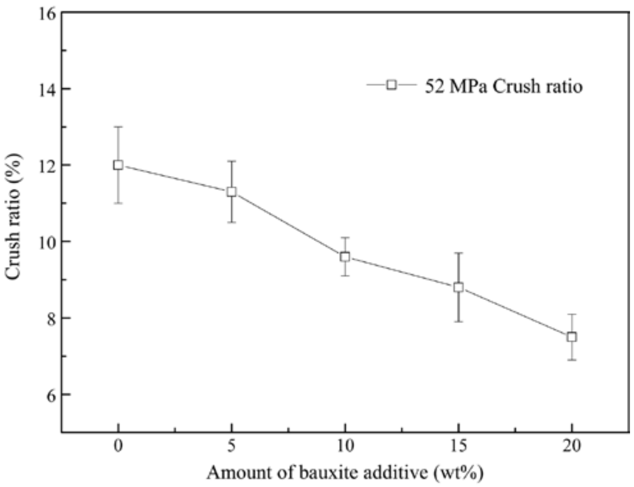

Figure 2: The crush ratio under 52 MPa pressure of the proppants sintered at 1200°C with different amounts of the bauxite additive.

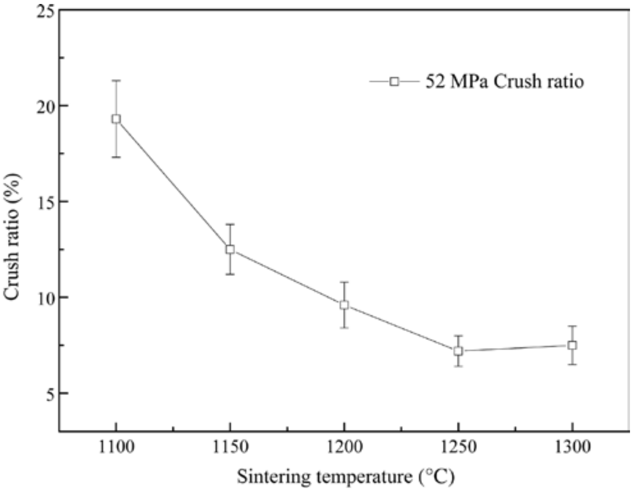

Figure 3: The crush ratio under 52 MPa pressure of the proppants sintered at different temperatures.

which met the operational requirements of CBM wells under 52 MPa (crush ratio ≤ 10%, according to the Petroleum and Gas Industry Standard SY/T 5108-2014). In consideration of the economic and environmental benefits, 10 wt% additives were selected for the preparation of the proppants, and a better performance was also obtained by the following optimization of sintering technology.

Sintering is one of the most important processes affecting the microstructure, phase composition, mechanical strength, and density of the obtained proppants [12–15]. The ideal proppants should be strong enough to resist closure pressure, and at the same time, have a low enough density to be carried easily into the cracks [16]. Figure 3 shows the crush ratio of the 40/70 mesh proppants sintered at different temperatures

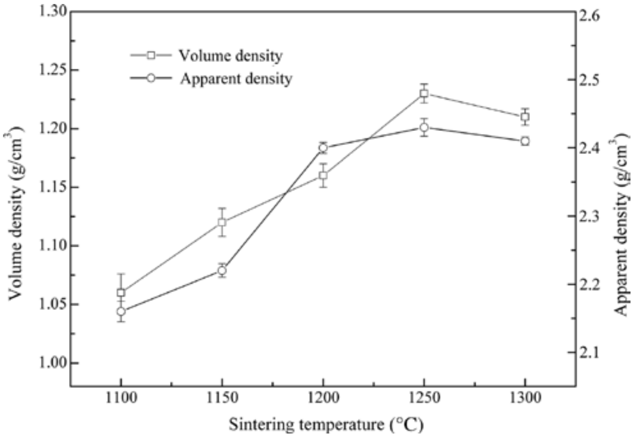

Figure 4: The packing density and apparent density of proppants sintered at different temperatures.

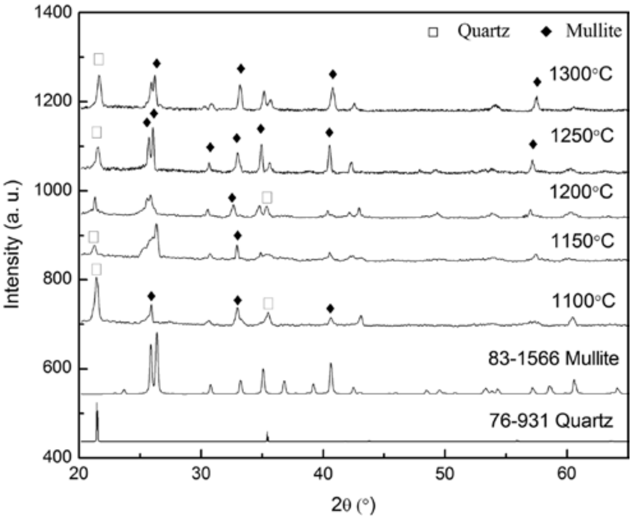

Figure 5: The XRD patterns of proppants at different sintering temperatures.

with 10 wt% additives under 52 MPa closure pressure. As can be seen, the crush ratio decreased as the sintering temperature increased and then remained steady (about 7.2%) when the temperature reached 1250°C. Moreover, when the sintering temperature was higher than 1300°C, the particles aggregated together and could not be applied to hydraulic fracturing.

The packing density and the apparent density of the proppants as a function of sintering temperature are shown in Figure 4. As can be seen, the highest packing density of 1.23 g/cm^3 and the highest apparent density of 2.42 g/cm^3 were obtained at the sintering temperature of 1250°C. These data agreed well with the crush-ratio results for the proppants. Compared with the bauxite-sintered proppants [17, 18], the samples obtained in the current

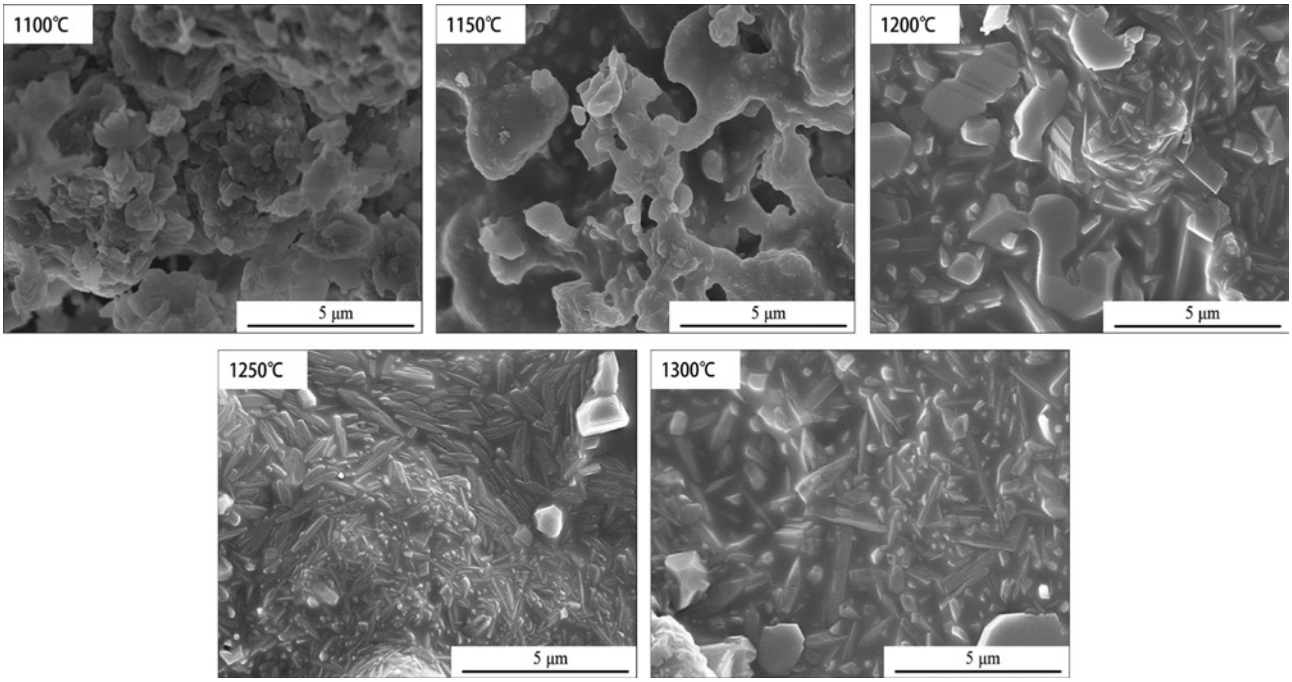

Figure 6: The SEM images of the proppants at different sintering temperatures.

study had a low cost with a lower density, although their crush ratios were somewhat high within a reasonable range of operational requirements for CBM wells. The low cost resulted mainly from the cheap starting materials of gangue and from the lower sintering temperatures.

Figure 5 shows the XRD patterns of the proppants sintered at different temperatures. At 1100°C, the proppants had a few peaks corresponding to the quartz phase (PDF No. 76-931 SiO_2); with the increase of sintering temperature, the peaks at 25.7° and 26.0° associated with the mullite crystals (PDF No. 83-1566 $3Al_2O_3 \cdot 2SiO_2$) were generally enhanced, whereas the quartz-related peak located at 22.5° started scattering. After 1250°C, mullite-related diffraction was clearly visible.

Figure 6 shows the scanning electron microscopy (SEM) photos of the proppants sintered at different temperatures. With the increase in sintering temperature, the raw materials of the proppants began to melt and formed the amorphous glass phase after 1150°C; the liquid phase also generally increased. The speeds of diffusion and flow-mass transfer increased, and the liquid filled the gap among the particles, whereas the particles flowed in the liquid phase, and the rearrangement occurred among the particles. In fact, the embryos of the mullite and quartz formed gradually before 1100°C, which were embedded in the amorphous matrix. Song et al. found that the presence of liquid phase benefited the formation of acicular mullite [19]. The quartz phases supposed to be in the microstructure were dispersed as the embryos of the mullite in the amorphous phase [20], and the particles consistently transmitted to the mullite embryos by liquid-phase mass transfer, resulting in the growth of mullite grains to form the fine acicular, together with the recrystallization of the quartz phase. This phenomenon was confirmed by the XRD results with the significant increase of mullite peaks. At temperatures of up to 1250°C, the small mullite grains dissolved into the liquid phase and were transmitted into the large ones by liquid-phase mass transfer. These mullite crystals increased in size within the liquid phase through a dissolution and reprecipitation process. A higher temperature provided a stronger driving force for the crystal growth of mullite, and the grains grew from small-scale (fine acicular-like) shapes to thicker, large-scale, rod-like shapes. After 1300°C, more liquid was produced, and the mullite continued to grow. The microstructure of the mullite crystals presented great dependence on the sintering temperature and duration. Afterwards, the proppants bonded together and could not be used for the hydraulic fracturing.

During the sintering process described previously, phase evolution was related to the following reactions (1)–(4) [10]. The densification of the proppants occurred because the progressive formation of the liquid phase cemented the matrix with the consequent reduction of fissures and cracks. The viscous flow mechanism of the liquid phase promoted the intense arrangement of the rod-like mullite grains and residual quartz in the matrix, and the interlocking of crystals in the interfaces of the two different phases resulted in the decrease of grain boundary between the pores and gaps [21, 22]. The strength of the proppants was strongly influenced by porosity, and the stress at the pores of the proppants was three times larger than that of the matrix, because the source of the cracks usually started at the position of the pores [23]. In addition, liquid filling prevented crack growth and enhanced the strength of the proppants. During the fracture process, the strain energy by the loading system provided the energy to break the structure bonds of the proppants, and no crack growth was possible unless the stress intensity at the crack tip exceeded the critical stress of proppants [24]. However, when closure stress reached the critical value, the proppants promoted the propagation and growth of cracks and finally fractured. The rod-like mullite hindered the growth of internal micro-cracks, just as the fiber-toughening effects improved the toughness and the strength of ceramics.

$$\begin{aligned}&Al_2O_3 + 3SiO_2 \xrightarrow{1067\sim1100°C} Al_2O_3 \cdot 2SiO_2(\text{mullite embryo})\\&\quad + SiO_2(\text{amorphous})\end{aligned} \tag{1}$$

$$\begin{aligned}&Al_2O_3 \cdot 2SiO_2(\text{mullite embryo}) \xrightarrow{1150\sim1200°C}\\&\quad Al_2O_3 \cdot 2SiO_2(\text{acicular mullite})\end{aligned} \tag{2}$$

$$\begin{aligned}&Al_2O_3 \cdot 2SiO_2(\text{acicular mullite}) \xrightarrow{1250\sim1300°C}\\&\quad Al_2O_3 \cdot 2SiO_2\ (\text{rodlike mullite})\end{aligned} \tag{3}$$

$$\begin{aligned}&SiO_2(\text{amorphous}) \xrightarrow{1150\sim1200°C} SiO_2(\text{quartz embryo})\\&\quad \xrightarrow{1250\sim1300°C} SiO_2(\text{quartz cube})\end{aligned} \tag{4}$$

4 Conclusions

In this work, mullite-quartz proppants sintered at 1250°C presented the best performance with a packing density of 1.23 g/cm^3, an apparent density of 2.42 g/cm^3, and a crush ratio of 7.2%, which met the 52 MPa operational requirements of CBM wells. The viscous flow mechanism of the liquid phase formed during the sintering process promoted the arrangement of grains, thus benefiting the densification and the strength of proppants. The viscous flow mechanism of the liquid phase also promoted the intense arrangement of the rod-like mullite grains and the residual quartz in the matrix, and the interlocking of crystals in the interfaces of the two different phases resulted in the enhanced strength of the proppants.

Acknowledgments: This work was supported by the Scientific and Technological Innovation Programs of Higher Education Institutions in Shanxi (Grant No. 2016-59), the Talents Training Project of Shanxi Graduate Joint Training Base (Grant No. 2017JD33), and the Shanxi Province Science Foundation (Grant No. 201601D102019). The authors also thank LetPub (www.letpub.com) for its linguistic assistance during the preparation of this manuscript.

References

[1] Gao L, Mastalerz M, Schimmelmann A. In *Coal Bed Methane – From Prospect to Pipeline*, Thakur P, Schatzel S, Aminian K, Eds., Elsevier Inc.: Amsterdam, 2014, pp 7–29.
[2] Lu S, Cheng Y, Qin L, Li W, Zhou, H, Guo H. *Int. J. Min. Sci. Technol.* 2015, 25, 819–825.
[3] Song D, Liu Z, Wang E, Qiu L, Gao Q, Xu Z. *Int. J. Rock. Mech. Min.* 2015, 78, 230–239.
[4] Zhao J, Liu Z, Li Z. *Mater. Lett.* 2015, 152, 72–75.
[5] Zhang D, Fan G, Ma L, Wang X. *Int. J. Coal Geol.* 2011, 86, 190–196.
[6] Gu M, Dao E, Mohanty KK. *Fuel* 2015, 150, 191–201.
[7] Dong Z, Xia J, Fan C, Cao J. *Constr. Build. Mater.* 2015, 100, 63–69.
[8] Kakali G, Perraki T, Tsivilis S, Badogiannis E. *Appl. Clay. Sci.* 2001, 20, 73–80.
[9] Xie Z, Xi Y. *Cem. Concr. Res.* 2001, 31, 1245–1249.
[10] Wang CL, Ni W, Zhang SQ, Wang S, Gai GS, Wang WK. *Constr. Build. Mater.* 2016, 104, 109–115.
[11] Yu-Ming T, Peng-Fei Z, Xiang-Chen K, Ai-Ping L, Kai-Yue W, Yue-Sheng C, Zhan-Gang L, De-Fu LV. *Sci. Sinter.* 2015, 47, 273–378.
[12] Liu LX, Niu RD, Jin HY, Lv BQ, Liu S. *Mater. Sci. Forum* 2012, 727, 69–72.
[13] Smith RJ, Loscutova JR, Whitsitt EA, Coker CE, Barron AR, Wiesner M, Costantion SA, Bordia RK. Composition and method for making a proppant. U.S. Patent Application 2013, 8298667
[14] Tong YP, Wang HX, Wang QF. *Appl. Mech. Mater.* 2013, 438–439, 207–210.
[15] Liu Z, Zhao J, Li Y, Zeng Z, Mao J, Peng Y, He Y. *Mater. Lett.* 2016, 171, 300–303.
[16] Lee DS, Elsworth D, Yasuhara H, Weaver JD, Rickman R. *J. Pet. Sci. Eng.* 2010, 74, 67–76.
[17] Zhao P, Tian Y, Liu A, Kong X, Chai Y, Li Z, Bai P. *China's Refractories* 2015, 24, 36–41.
[18] Ma X, Tian Y, Zhou Y, Wang K, Chai Y, Li Z. *Mater. Lett.* 2016, 180, 127–129.
[19] Song H, Coble RL. *J. Am. Ceram. Soc.* 2010, 73, 2077–2085.
[20] Kamseu E, Braccini S, Corradi A, Leonelli C. *Adv. Appl. Ceram.* 2009, 108, 338–346.
[21] Chen CY, Lan GS, Tuan WH. *J. Eur. Ceram. Soc.* 2000, 20, 2519–2525.
[22] German RM. *Sci. Sinter.* 2006, 38, 27–40.
[23] Kong X, Tian Y, Chai Y, Zhao P, Wang K, Li Z. *Ceram. Int.* 2015, 41, 4294–4300.
[24] Loehman RE, Claus AC. *Characterization of Ceramics*, 1st ed., Harbin Institute of Technology Press: Harbin, 2014.